Study on Weather Aging of Nitrile Rubber Composites Containing Imidazolium Ionic Liquids

Anna Marzec,*[2] *Anna Laskowska*,[1] *Gisele Boiteux*,[2] *Marian Zaborski*,[2] *Olivier Gain*,[2] *Anatoli Serghei*[2]

Summary: Weather aging of nitrile rubber composites containing hydrophilic 1-ethyl-3-methylimidazolium thiocyanate (EMIM SCN) and hydrophobic 1-ethyl-3-methylimidazolium bis(trifluoromethylsulfonyl)imide (EMIM TFSI), and 1-allyl-3-methylimidazolium bis(trifluoromethylsulfonyl)imide (AMIM TFSI) ionic liquids was investigated. The mechanical properties at small (dynamic mechanical analysis) and high deformation (tensile test), the hardness and the electrical properties were measured before and after the aging process. It was found that the presence of hydrophobic ionic liquids in the nitrile rubber enhanced the retention of their mechanical properties (tensile strength, stiffness) and slightly reduced surface defects (as determined by scanning electron microscopy), thereby retarding the aging of rubber composites. However, the presence of hydrophilic EMIM SCN in the composite accelerated the degradation of the studied materials because of its high crosslinking activity during the aging process. The electrical studies showed also lower stability of hydrophilic ionic liquid (EMIM SCN) in the studied nitrile matrix (leaking effects) compared to the hydrophobic one (EMIM TFSI, AMIM TFSI).

Keywords: acrylonitrile-butadiene rubber; elastomer composites; ionic conductivity; ionic liquids; mechanical properties; weather aging

Introduction

Nitrile rubber is a type of synthetic rubber that is obtained by the low-temperature polymerization of butadiene and acrylonitrile. Nitrile rubber is mainly used for manufacturing oil-resistant rubber products, which are widely used in the automotive and aerospace industries, oil exploration, petrochemicals, textiles, wire and cable, printing and food packaging.[1] Elastomeric materials are especially sensitive to oxidative degradation. During a long period of service most polymers and their products gradually lose their useful properties as a result of polymer chain degradation. During their outdoor exposure, elastomers containing diene units (C=C) are subjected to different environmental factors.[2–5] Oxygen, high temperature and UV radiation are among the most significant factors degrading polymeric materials by chemical modification at the molecular scale because of their sensitivity towards oxidation.[6–11] After a certain period of time, an oxidized skin is formed on the surface of polymer composites; these oxidative coatings act as stress concentrators. The formation of oxidized groups involves chain scissions and the formation of new covalent bonds between chains (crosslinking), resulting in the deterioration of the physical and mechanical properties of rubber materials.[12–15] The competition between these two opposing phenomena (chain scissions and crosslinking) depends on several factors including the conditions of the aging and the chemical structure of

[1] Technical University of Lodz, Institute of Polymer and Dye Technology, Stefanowskiego 12/16, 90924 Lodz, Poland
Fax: +48(42) 636 25 43;
E-mail: marzec.anna@hotmail.com
[2] University of Lyon, Université Claude Bernard Lyon1, Ingénierie des Matériaux Polymères, UMR CNRS 5223, 43 Bd du 11 Novembre 1918, 69622 Villeurbanne, France

the polymer.[16] Some indicators of polymer oxidation are changes in the mechanical properties (tensile strength, hardness), changes in the weight and color and a change in the glass temperature T_g.[17] Not only the chemical structure of the rubber materials is important with respect to its stability but also additives such as fillers, curatives (peroxides or sulfur-based systems), accelerators, dyes, pigments, modifiers, etc. Few articles have dealt with the influence of reinforcing fillers such as carbon black[18,19] and nano-clay[20] on the thermal aging of elastomer composites. In many cases, dyes and pigments can also have a marked influence on the thermal and photochemical stability of the polymer material.[21,22] Ionic liquids have found use in polymers as plasticizers,[23] antistatic additives[24] and have been used to enhance the ionic conductivity and the mechanical and thermal properties of the polymer composites, as well as to improve the filler dispersion (e.g., carbon nanotubes,[25–27] carbon black,[28,29] or silica[30,31]) in hydrophobic matrices. Some reports have described the thermal degradation of polychloroprene rubber (CR) composites based on unmodified and ionic liquid 1-butyl-3-methylimidazolium bis(trifluoromethylsulfonyl)imide (BMIM TFSI) modified multi-walled carbon nanotubes (MWCNTs).[32,33] The authors concluded that the composites with modified MWCNTs exhibited higher mechanical properties (tensile modulus, hardness) and thermal stability than the composites with unmodified MWCNTs. ILs were also found to have multifunctional roles (as antioxidants, as coupling agents) in the composites. However, a lack of scientific information exists about weather aging the rubber composites with ionic liquids, which is an important issue to predict the polymer lifetime because this aging is induced by light, oxygen, ozone, moisture and any combination of these individual agents. The current work is aimed at studying rubber/ionic liquids composites as a continuation of our previous results.[34] The aim of the present paper was to characterize the changes that occur during weather aging of acrylonitrile-butadiene rubber (NBR) composites filled with hydrophilic 1-ethyl-3-methylimidazolium thiocyanate (EMIM SCN) and hydrophobic 1-ethyl-3-methylimidazolium bis(trifluoromethylsulfonyl)-imide (EMIM TFSI), and 1-allyl-3-methylimidazolium bis(trifluoromethylsulfonyl)-imide (AMIM TFSI) ionic liquids.

Materials and Methods

Acrylonitrile-butadiene rubber NBR (Perbunan 28-45F) containing 28 wt% of acrylonitrile (Lanxess, GmbH). The Mooney viscosity was (ML1 + 4(100 °C):45). NBR rubber was cured using a conventional sulfur (Siarkpol, Poland)-based crosslinking system in the presence of mercaptobenzothiazole as an accelerator (MBT Lanxess, GmbH). Zinc oxide (Lanxess, GmbH) and stearic acid (Sigma Aldrich, GmbH) were used as activators in the sulfur vulcanization. Hydrophilic fumed silica Aerosil 380 (Evonik Degussa, GmbH) was used as a reinforcing filler. The ionic liquids: 1-ethyl-3-methylimidazolium bis(trifluoromethylsulfonyl)imide (EMIM TFSI), 1-allyl-3-methylimidazolium bis(trifluoromethylsulfonyl)imide (AMIM TFSI), and 1-ethyl-3-methylimidazolium thiocyanate (EMIM SCN) were provided by Sigma Aldrich. The rubber mixture consisted of the following: NBR (100 phr), sulfur (2 phr), mercaptobenzothiazole (2 phr), zinc oxide (5 phr), stearic acid (1 phr), Aerosil 380 (30 phr) and ionic liquid (5 phr). The preparation of the rubber mixtures was performed by following a two-step procedure. Homogenization of the rubber and SiO_2 filler mixed with the ionic liquid was performed in an internal mixer (Brabender Measuring Mixer N50). The rubber compounds were processed at a rotor speed of 50 rpm and an initial temperature of 50 °C. Subsequently, the compounded rubbers were then milled with sulfur, mercaptobenzothiazole, zinc oxide and stearic acid in a laboratory rolling mill (roll dimensions: D = 200 mm, L = 450 mm).

The stress-strain tests before and after aging were performed with a universal material testing machine (Zwick model 1435) with a crosshead speed of 500 mm/min, according to the standard PN-ISO 37-2005. To measure the mechanical properties, five different dumbbell-shaped specimens were punched from each rubber sample (mean ± std). The tensile strength and elongation at break were measured at room temperature. The crosslinking density in the vulcanized network was determined using the method of equilibrium swelling. The vulcanizates were subjected to equilibrium swelling in toluene for 48 h at room temperature. The swollen samples were then weighed on a torsion balance, dried in a dryer at a temperature of 60 °C to a constant weight and reweighed after 48 h. The crosslinking density was determined on the basis of the Flory–Rehner equation.[35] The surface morphologies of the composite before and after aging were characterized using scanning electron microscopy with a Zeiss SEM microscope. Prior to the measurements, the samples were coated with carbon. Dynamic mechanical analysis of the composites was performed in a Dynamic Mechanical Analyzer (TA Instrument Q 800 DMA, USA). The storage modulus (E′) and loss tangent (tan δ) were measured in tension mode in the temperature range of -90 to 100 °C at a frequency of 10 Hz and a heating rate of 2 °C/min. Dielectric measurements were conducted with broadband dielectric spectroscopy (Novocontrol alpha analyzer, Hundsagen, Germany) in the frequency range from 10^{-1} to 10^{7} Hz at room temperature. The samples were placed between two copper electrodes with diameters of 20 mm. Weather aging was carried out using a Weather-Ometer (Atlas; Ci4000). The measurement lasted for 216 h and consisted of two alternately repeating segments with the following parameters: daily segment (radiation intensity 0.4 W/m^2, temperature 60 °C, humidity 60%, duration 4 h), night segment (no UV radiation, temperature 50 °C, humidity 50% duration 3 h). The samples were controlled every 24 hours. The aging coefficient S was calculated according to the following relationship: $S = [TS_A \times Eb_A]/[TS_B \times Eb_B]$, where TS corresponds to the tensile strength, Eb to the elongation at break, and TS_A and Eb_A correspond to the values of the TS and Eb after aging, respectively. The color of the obtained vulcanizates was measured by means of a CM-3600d spectrophotometer. The instrument provided the color in the terms of the CIE L*a*b* color space system. In this color space, L represented the lightness (or brightness), a and b were color coordinates, where +a* was the red direction, -a* was the green direction, +b* was the yellow direction, and –b* was the blue direction. Moreover, changes in individual components allowed to estimate the total change of color E. The spectral range of the apparatus was 360–740 nm, where the change of color ΔE was calculated by the equation below.

$$\Delta E = \sqrt[2]{(\Delta L)^2 + (\Delta a)^2 + (\Delta b)^2}$$

ΔL corresponds to the difference in the brightness intensity between light and dark, Δa corresponds to the difference of intensity between green and red, Δb corresponds to the difference of intensity between blue and yellow, and the Δ symbol implies the difference in the colors of the samples before and after aging. The spectra of the vulcanizates were recorded with a Nicolet 700 IR spectrophotometer.

Results and Discussion

Tensile properties are commonly used to measure the degradation (damage) of elastomers. The NBR/SiO_2/AMIM TFSI and NBR/SiO_2/EMIM TFSI samples before aging exhibited higher strain and elasticity compared to the NBR/SiO_2/EMIM SCN and neat NBR/SiO_2 composites, as previously described.[34] For samples containing EMIM TFSI and AMIM TFSI, the strain at break was found to be approximately 699% and 695% before aging. The mechanical behavior of these materials was different after 24 h of aging, with a lower elongation

at break of approximately 25% and 26% for EMIM TFSI and AMIM TFSI, respectively. The decrease in the elongation at break for the neat NBR/SiO_2 was the most pronounced and reached around 35%. The reason for the low elasticity values in the NBR/SiO_2 and NBR/SiO_2/IL composites was most likely due to the large increase in the composite crosslink density during the aging process (Figure 2 b).

From the results in Figure 1 (a, b, c) a better retention of the mechanical properties was observed in composites using EMIM TFSI and AMIM TFSI (higher S coefficient) as opposed to NBR/SiO_2 and NBR/SiO_2/EMIM SCN. Figure 1 (a, b) shows the change in the tensile strength and elongation at break of the composites during the aging process. The tensile strength decreases very rapidly for to

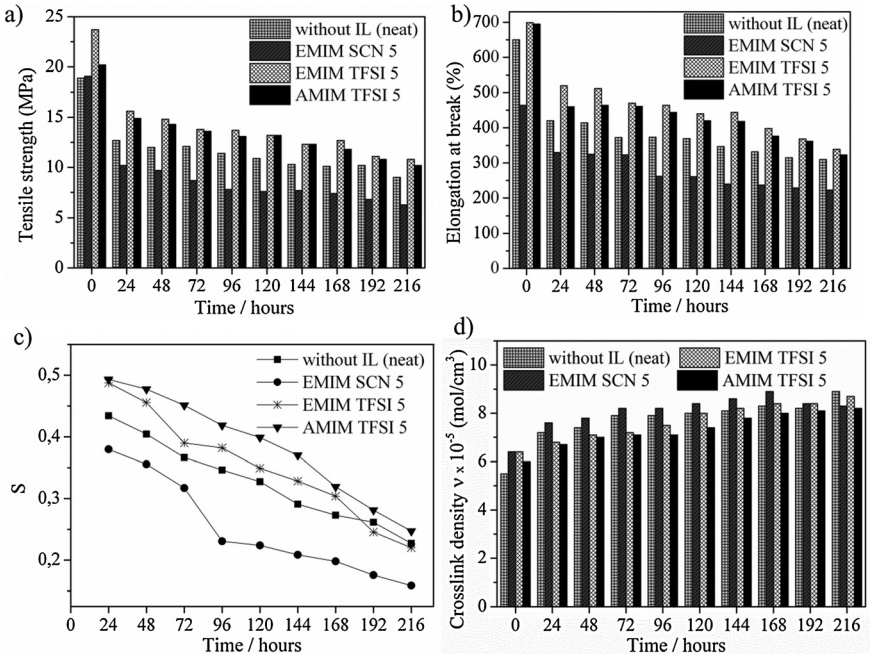

Figure 1.
Tensile strength (a), elongation at break (b), aging coefficient S (c) and crosslink density ν (d) as a function of the aging time of the NBR composites.

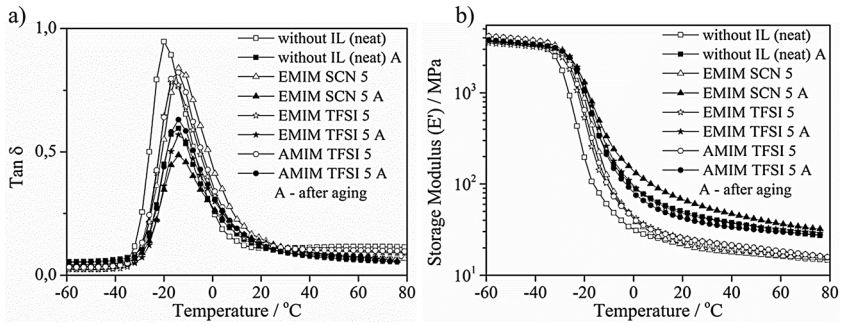

Figure 2.
Temperature dependence of the loss tangent tan δ (a) and the storage modulus E′ (b) values at 10 Hz for the NBR/SiO_2 and NBR/SiO_2/IL composites before and after aging for 216 h.

NBR/SiO_2 and NBR/SiO_2/EMIM SCN with an increase in the exposure time. However, the decrease in the strain at break of samples with EMIM TFSI and AMIM TFSI was not as rapid as it was observed for NBR/SiO_2 and NBR/SiO_2/EMIM SCN composites. This is most likely due to the lower tendency to the crosslinks formation in the presence of the hydrophobic ILs in nitrile composites, during outdoor exposure. The EMIM SCN showed a high crosslinking activity during the aging process what increased brittleness of the samples and a faster degradation of the polymer. The effect of the weather aging time on the tensile modulus (stress at 100%, 200% and 300% elongation) of the NBR/SiO_2 and NBR/SiO_2/IL composites is shown in Table 1. The modulus are related to the stiffness and cross-linking density (Figure 2 d) of the rubber compounds. It can be observed that the stress modulus of the compounds increased with the increasing aging time; this increase was especially

Table 1.
The results of the tensile properties as a function of the aging time.

NBR composites	Time [a] hours	SE_{100} [b] MPa	SE_{200} [c] MPa	SE_{300} [d] MPa	TS[e] MPa	Eb[f] %	Hardness Shora A
neat	–	2.2 ± 0.1	3.3 ± 0.1	4.0 ± 0.3	18.9 ± 1.6	650 ± 12	76
neat	24	2.6 ± 0.2	5.1 ± 0.2	6.5 ± 0.3	12.0 ± 2.0	420 ± 10	79
neat	48	3.4 ± 0.2	5.3 ± 0.1	7.8 ± 0.3	11.2 ± 1.1	414 ± 8	81
neat	72	3.1 ± 0.1	5.4 ± 0.2	8.8 ± 0.4	12.1 ± 1.4	372 ± 11	82
neat	96	3.4 ± 0.2	5.5 ± 0.3	8.7 ± 0.3	11.4 ± 1.2	373 ± 12	81
neat	120	3.4 ± 0.3	5.9 ± 0.3	9.8 ± 0.4	10.9 ± 1.2	369 ± 7	82
neat	144	4.1 ± 0.2	7.2 ± 0.2	11.3 ± 0.3	10.3 ± 1.0	347 ± 9	82
neat	168	4.3 ± 0.2	7.3 ± 0.3	11.0 ± 0.4	10.1 ± 0.9	332 ± 10	82
neat	192	4.4 ± 0.3	7.1 ± 0.3	10.8 ± 0.3	10.2 ± 2.0	315 ± 11	83
neat	216	4.5 ± 0.3	7.2 ± 0.3	10.7 ± 0.2	9.0 ± 1.2	310 ± 9	83
EMIM SCN	–	3.0 ± 0.1	5.4 ± 0.2	7.2 ± 0.2	19.1 ± 1.7	464 ± 13	77
EMIM SCN	24	3.3 ± 0.2	5.1 ± 0.2	7.5 ± 0.3	10.2 ± 2.0	330 ± 5	78
EMIM SCN	48	3.5 ± 0.2	4.7 ± 0.3	7.3 ± 0.2	9.7 ± 1.1	325 ± 7	80
EMIM SCN	72	3.5 ± 0.2	5.4 ± 0.1	8.1 ± 0.3	8.7 ± 0.9	323 ± 14	82
EMIM SCN	96	3.7 ± 0.1	5.6 ± 0.2	–	7.8 ± 0.8	262 ± 9	82
EMIM SCN	120	3.8 ± 0.1	5.9 ± 0.4	–	7.6 ± 0.7	261 ± 8	83
EMIM SCN	144	4.4 ± 0.2	6.5 ± 0.2	–	7.7 ± 1.0	240 ± 7	83
EMIM SCN	168	4.7 ± 0.2	7.4 ± 0.3	–	7.4 ± 1.2	237 ± 6	82
EMIM SCN	192	4.6 ± 0.3	7.5 ± 0.4	–	6.8 ± 2.0	229 ± 6	80
EMIM SCN	216	4.6 ± 0.2	7.4 ± 0.3	–	6.3 ± 1.1	223 ± 5	79
EMIM TFSI	–	2.3 ± 2.0	3.1 ± 0.1	4.3 ± 0.3	23.7 ± 2.0	698 ± 15	73
EMIM TFSI	24	3.1 ± 2.0	4.2 ± 0.3	6.0 ± 0.3	15.6 ± 2.2	520 ± 12	75
EMIM TFSI	48	3.4 ± 0.3	4.3 ± 0.2	7.4 ± 0.2	14.8 ± 2.1	512 ± 13	77
EMIM TFSI	72	3.5 ± 0.1	4.1 ± 0.1	5.5 ± 0.1	13.8 ± 2.0	470 ± 14	80
EMIM TFSI	96	3.7 ± 0.2	5.3 ± 0.3	7.4 ± 0.2	13.7 ± 1.3	464 ± 11	80
EMIM TFSI	120	3.6 ± 0.2	5.3 ± 0.1	7.6 ± 0.1	13.9 ± 1.0	440 ± 12	80
EMIM TFSI	144	4.2 ± 0.1	5.6 ± 0.2	8.9 ± 0.3	12.3 ± 1.3	444 ± 13	81
EMIM TFSI	168	4.1 ± 0.2	6.1 ± 0.2	8.4 ± 0.3	12.7 ± 0.9	398 ± 10	83
EMIM TFSI	192	4.3 ± 2.0	6.5 ± 0.3	9.2 ± 0.2	11.1 ± 1.1	368 ± 11	82
EMIM TFSI	216	4.3 ± 0.3	6.8 ± 0.3	9.8 ± 0.4	10.8 ± 0.8	339 ± 7	83
AMIM TFSI	–	1.9 ± 0.1	2.5 ± 0.2	4.0 ± 0.2	20.2 ± 1.4	695 ± 14	73
AMIM TFSI	24	3.3 ± 0.2	4.4 ± 0.3	5.4 ± 0.3	15.1 ± 1.6	460 ± 9	75
AMIM TFSI	48	3.1 ± 0.3	4.1 ± 0.2	5.7 ± 0.3	14.3 ± 1.3	464 ± 13	78
AMIM TFSI	72	3.4 ± 0.1	4.9 ± 0.3	6.8 ± 0.2	13.6 ± 1.1	461 ± 10	80
AMIM TFSI	96	3.4 ± 0.1	5.1 ± 0.2	7.6 ± 0.3	13.1 ± 1.2	444 ± 9	81
AMIM TFSI	120	3.5 ± 0.2	4.9 ± 0.1	7.0 ± 0.2	13.2 ± 1.0	420 ± 8	80
AMIM TFSI	144	3.5 ± 0.3	5.7 ± 0.3	7.8 ± 0.3	12.3 ± 1.3	418 ± 10	80
AMIM TFSI	168	3.7 ± 0.2	5.6 ± 0.2	8.3 ± 0.3	11.8 ± 1.1	376 ± 13	81
AMIM TFSI	192	4.0 ± 0.2	5.8.9 ± 0.1	9.2 ± 0.1	10.8 ± 0.8	362 ± 13	82
AMIM TFSI	216	4.1 ± 0.3	6.0 ± 0.3	9.0 ± 0.3	10.2 ± 1.2	323 ± 9	81

[a] Time – weathering time. [b] SE_{100}–modulus at 100% elongation. [c] SE_{200}–modulus at 200% elongation. [d] SE_{300}–modulus at 300% elongation. [e] TS – tensile strength. [f] Eb – elongation at break.

pronounced for the NBR/SiO_2 and NBR/SiO_2/EMIM SCN composites. Furthermore, decrement in the stress at 300% elongation of NBR/SiO_2/EMIM SCN was observed when the irradiation was longer than 96 h. These changes were directly associated with changes in the original crosslinked structure, i.e., main chain scission and crosslinking.[36] The formation of photo-products and a crosslinked network in the studied materials during aging led to an increase in the stiffness of the composites. As a consequence, the materials become more brittle, lose flexibility and their surface get cracked what results in a decrease in mechanical strength of the samples. The crosslink densities increased for all the samples in the studied aging time. The crosslink density was found to be the highest for NBR/SiO_2/EMIM SCN composite. It seems that this IL most likely acts as an accelerator for the formation of crosslinks in NBR sulfur-based systems upon aging. The hardness (Shore A) values of the unaged and aged composites are reported in Table 1. With the increasing aging time, an increment in the hardness was found for all studied composites, which is correlated with an increase brittleness of the samples due to an increase crosslink density.[33,37,38] The lowest values of hardness during weathering were obtained for NBR/SiO_2/AMIM TFSI, which is in good agreement with its the lowest crosslink density, as determined from the swelling measurements. For all composites, the difference between the mechanical responses of the unaged and aged materials is most likely due to the formation of an oxidative layer during the thermal- and photo-aging. In fact, the hardening at the surface during irradiation is linked to the formation of a crosslinked network, and the oxidized products hinder the mobility of the macromolecules.[39,40]

These constraints at the surface of the material imply the formation of cracks during elongation, which leads to a lower strain at break compared to the unaged material. It is well-known that the change in the mechanical properties of materials during aging is due to the changes in the conformation of the macromolecular chains. During the outdoor exposure of rubber, the formation of three-dimensional networks by means of crosslinks leads to a decrease in the chain mobility and a decrease in the loss factor maximum (tan δ).[41] A change in T_g of the composites, as observed from the DMA, is also a sign of crosslinking/scission. An up-shift in T_g indicates crosslinking, and a down-shift in T_g indicates chain scission.[17] Figure 2 and Table 2 show the change of tan δ and the ratio E′ of the studied materials before and after 216 h of irradiation.

After 216 hours of the weather aging test, the tan δ of all composites decreased and T_g was shifted to higher temperatures. Only for the EMIM SCN composite was a slight reduction in T_g observed, which was most likely due to the intensification of the chain scission process. Moreover, for NBR/SiO_2 and NBR/SiO_2/IL, a decrease in tan δ

Table 2.
DMA properties of the NBR composite after aging for 216 h.

NBR composites	Time [a] hours	E′ [b] MPa 25 °C	E′ MPa 40 °C	tan δ [c]	Value T °C
neat	–	21.3	18.6	0.95	−16.2
neat	216	45.6	37.6	0.60	−15.1
EMIM SCN	–	20.1	17.9	0.85	−13.1
EMIM SCN	216	60.3	46.9	0.57	−14.2
EMIM TFSI	–	24.3	21.1	0.80	−15.6
EMIM TFSI	216	43.8	37.0	0.48	−14.0
AMIM TFSI	–	24.1	21.2	0.85	−15.4
AMIM TFSI	216	39.1	33.7	0.63	−14.3

[a] Time – weathering time. [b] E′ – storage modulus. [c] tan δ – loss tangent.

was observed, which suggests variations in the change of the visco-elastic properties during outdoor aging of the NBR-based materials. The lowest changes after the 216 h exposure were found for the NBR/SiO_2/AMIM TFSI composite; tan δ values changed from 0.85 to 0.63, which is in good agreement with previously described results. Considering the unaged samples, IL-filled composites demonstrate a lower tan δ than neat NBR/SiO_2 due to the higher number of crosslinks. After a 216 h irradiation, we observed increases in the E′ and decreases in the tan δ of all the aged samples compared to their unaged counterparts, which is mainly due to the increase in the crosslinking density.[42] A significant increase in the storage modulus was observed for NBR/SiO_2/EMIM SCN (60.3 MPa at room temperatutre), whereas that for NBR/SiO_2, the E′ reached 45.6 MPa under the same temperature conditions. However, the increase in the E′ value of composites containing AMIM TFSI (38%, at room temperature) and EMIM TFSI (45%, at room temperature) was lower in the comparison to the NBR/SiO_2 sample (54%, at room temperature).

Table 3 illustrates the AC conductivity of the studied samples before and after the aging process. The ionic conductivities of unaged NBR/SiO_2 and NBR/SiO_2/EMIM SCN were found to be 3.6×10^{-10} $S \cdot cm^{-1}$ and 1.8×10^{-9} $S \cdot cm^{-1}$, respectively, whereas for the composites containing TFSI anion, NBR/SiO_2/EMIM TFSI and NBR/SiO_2/AMIM TFSI, the ionic conductivities were both 1.3×10^{-8} $S \cdot cm^{-1}$. However after an exposure time of 216 h, the conductivities of the neat NBR/SiO_2 and compounds with TFSI anion decreased. This can be explained through the increased crosslink density of aged rubber compounds, that affects T_g of the composites. The increase in T_g value results from lowered mobility of the polymer chains and may decrease the ionic conductivity of the composites. Contrary to the samples discussed up to this point, the conductivity of NBR/SiO_2/EMIM SCN shows a slight increase, up to 1.1×10^{-8} $S \cdot cm^{-1}$. This is most likely because of the hydrophilic nature of the liquid. Due to the action of factors such as temperature and light, the ionic liquid was probably leaked onto the surface of the composite, increasing its conductivity after aging test. This phenomenon was not observed for the composites filled with hydrophobic ionic liquids containing TFSI anion. Better stability in nitrile rubber may be provided by the compatibility of hydrophobic ILs with a hydrophobic polymer matrix and the interaction of the ILs with the functional groups of the polymer. Marwanta[43] reported a Raman study of NBR/EMIM TFSI composites that detected the existence of an interaction between the TFSI anion and the –CN group, which may be responsible for the improved compatibility of this type of ionic liquid with a polar matrix. Das[26] studied the coupling activity of 1-allyl-3-methylimidazolium chloride between diene elastomers and multi-walled carbon nanotubes. He concluded that the double bond present in the of 1-allyl-3-methylimidazolium chloride molecules was chemically linked with the double bond of the diene rubber molecules by sulfur bridges, thus providing superior mechanical and electrical properties. In our investigation 1-allyl-3-methylimidazolium bis(trifluoromethanesulfonyl) imide (AMIM TFSI) has a double bond attached to the imidazolium cation ring, which can exhibit similar behavior in nitrile rubber and improve the ionic liquid stability in the polymer matrix.

Table 3.
Ionic conductivity σ_{AC} after 216 h weathering for the NBR composites.

NBR composites	Time [a] hours	σ_{AC} [b] $S \cdot cm^{-1}$, 1 kHz, 25 °C
neat	–	3.6×10^{-10}
neat	216	9.7×10^{-11}
EMIM SCN	–	1.8×10^{-9}
EMIM SCN	216	1.1×10^{-8}
EMIM TFSI	–	1.3×10^{-8}
EMIM TFSI	216	4.6×10^{-9}
AMIM TFSI	–	1.3×10^{-8}
AMIM TFSI	216	8.8×10^{-9}

[a] Time – weathering time. [b] σ_{AC} – AC conductivity, 1 kHz, 25 °C.

Surface Analysis

Colorimetric studies in the CIE $L^*a^*b^*$ system provided information on the color characteristics of the composites after weather test (Figure 3). The coefficient ΔE defines to what extent the color of the samples changed during the 216 h exposure time. The obtained data indicated that the color of all the studied samples changed after 24 h of irradiation, especially that of the NBR/SiO_2/EMIM SCN composite. The significant change in color of this sample can be explained by the weak light stability of the 1-ethyl-3-methylimidazolium thiocyanate ionic liquid. The EMIM SCN salt is often yellow or orange in color and darkens upon extended exposure to sunlight. The thiocyanate ion is known to dimerize to thiocyanogen $(SCN)_2$ under chemically or electrochemically oxidative conditions in melt and then polymerize to polythiocyanogen $(SCN)_x$. Both thiocyanogen and polythiocyanogen are known to be photoactive.[44–46] Ionic liquids with the TFSI anion seem to not influence significantly on the surface color of the composites during irradiation, as the values of the ΔE coefficients in these samples were similar to those of the neat.

The micro-morphology and microstructures of the composites were investigated by scanning electron microscopy. Figure 4 presents the SEM photos of the NBR/SiO_2 and NBR/SiO2/AMIM TFSI composites before and after 216 h of the weather test. The vulcanizates before aging (4 a, d) are characterized by their smooth surface and uniform structure. A series of cracks of varying size appeared on the surface of the composites after the aging process. This is due to the rupture of the macromolecular network structure on the nitrile rubber surface or molecular chain crosslinking or degradation, thereby forming surface defects. In the case of NBR/SiO_2, significant changes in the surface morphology after aging were observed; the cracks are very prominent as a result of the surface oxidation. It is worthwhile to note that the pictures were taken at different areas of the composites. The SEM pictures of NBR/SiO_2/AMIM TFSI also showed surface defects, but they were not as serious as those in the NBR/SiO_2. In the composites containing ionic liquids, we noticed fewer but deeper cracks and areas that were almost free from damage. To confirm the post-aging chemical changes of the composites, they were analyzed using ATR-FTIR spectroscopy. After a 24 h aging, the changes in the analyzed spectra of the rubber/ionic liquid composites were slightly lower in comparison to those in the spectrum of NBR/SiO_2. Nevertheless, further differences between the aged (more than 24 h) composites were found to be marginal.

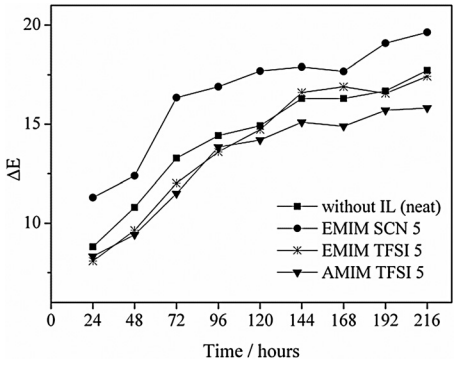

Figure 3.
Color difference (ΔE) of the nitrile composites containing ionic liquids after weather aging.

Conclusion

The weather aging of nitrile rubber composites was investigated and the effect of the presence of hydrophilic and hydrophobic ionic liquid was reported. The mechanical properties NBR/SiO_2 and NBR/SiO_2/IL at small (DMA) and high deformation (tensile test) were studied. The NBR/SiO_2/EMIM SCN composite subjected to the weather test displays the lowest values of elongation at break and tensile strength, as well as the highest stiffness (highest E′ modulus). This result can be explained by the fact that the hydrophilic liquid EMIM SCN not only accelerates the crosslinking

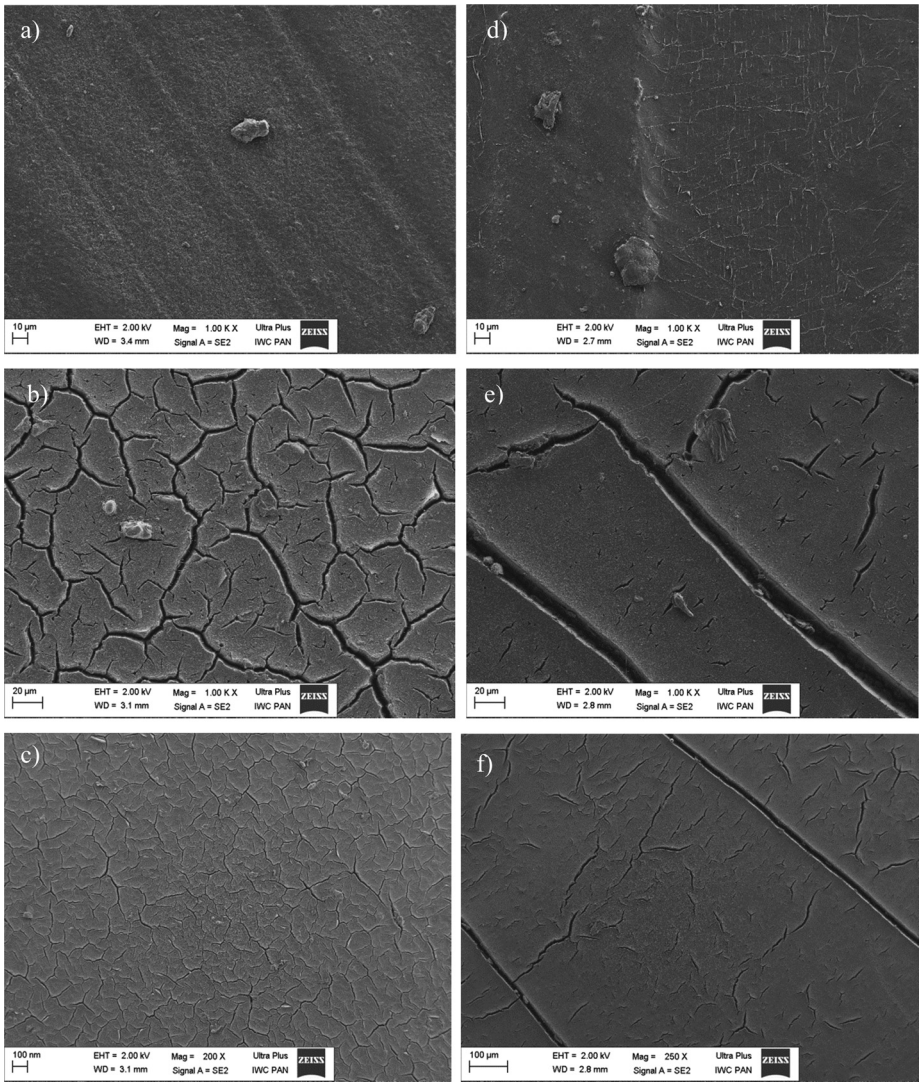

Figure 4.
SEM micrographs of (a) NBR/SiO_2 before aging, (b, c) NBR/SiO_2 after 216 h aging, (d) NBR/SiO_2/AMIM TFSI before aging, (e, f) NBR/SiO_2/AMIM TFSI after 216 aging.

during vulcanization but is also activated during aging, contributing to a faster degradation of the polymer. The smallest changes in the mechanical and visco-elastic (tan δ) properties after aging were shown by the rubber/ionic liquids composites with the TFSI anion, especially AMIM TFSI. Moreover, the study on the dependence of the electrical conductivity of the weather aging demonstrated a better stability of the hydrophobic IL (EMIM TFSI, AMIM TFSI) in the polymer matrix compared to the hydrophilic IL (EMIM SCN). The fracture morphology of the composites containing both types of ionic liquids showed less cracks and roughness on the surface than the control composite. Nevertheless, after aging, differences in the spectra of the NBR/SiO_2 and NBR/SiO_2/IL composites were found to be marginal. It

can be concluded that the studied hydrophobic ionic liquids, 1-ethyl-3-methylimidazolium bis(trifluoromethylsulfonyl)imide (EMIM TFSI) and 1-allyl-3-methylimidazolium bis(trifluoromethylsulfonyl)imide (AMIM TFSI) retarded the aging process of nitrile rubber composites exposed to outdoor conditions.

[1] C. A. Mahieux, D. Lehmann, A. des Ligneris, *Polym. Test* **2002**, *21*, 751.
[2] G. Mertz, F. Hassouna, P. Leclère, A. Dahoun, V. Toniazzo, D. Ruch, *Polym. Degrad. Stab.* **2012**, *97*, 2195.
[3] M. Piton, A. Rivaton, *Polym. Degrad. Stab.* **1996**, *53*, 343.
[4] C. Adam, J. Lacoste, J. Lemaire, *Polym. Degrad. Stab.* **1989**, *24*, 185.
[5] C. Adam, J. Lacoste, J. Lemaire, *Polym. Degrad. Stab.* **1989**, *26*, 269.
[6] P. O. Bussière, J. L. Gardette, J. Lacoste, M. Baba, *Polym. Degrad. Stab.* **2005**, *88*, 182.
[7] G. Y. Li, J. L. Koening, *Rubb. Chem. Technol.* **2005**, *78*, 355.
[8] S. W. Beavan, D. Philips, *Eur Polym. J* **1974**, *10*, 593.
[9] J. Lacoste, C. Adam, N. Siampiringue, J. Lemaire, *Eur. Polym. J.* **1994**, *30*, 443.
[10] M. Piton, A. Rivaton, *Polym. Degrad. Stab.* **1997**, *55*, 147.
[11] K. W. Ho, *J Polym. Sci.* **1986**, *24*, 2467.
[12] R. L. Pecsok, J. R. Shelton, J. L. Koenig, *Rubber Chem. Technol.* **1981**, *49*, 324.
[13] S. Yano, *Rubber Chem. Technol.* **1980**, *54*, 1.
[14] J. Lucki, B. Ranby, J. F. Rabek, *Eur Polym. J* **1979**, *15*, 1089.
[15] F. A. Bottino, A. R. Cinquegrani, G. Di Pasquale, L. Leonardi, A. Pollicino, *Polym. Test* **2004**, *23*, 405.
[16] E. Jubete, C. M. Liauw, K. Jacobson, N. S. Allen, *Polym. Degrad. Stab.* **2007**, *92*, 1611.
[17] T. Gates, The physical and chemical ageing of polymeric composites. In: R. Martin, (Ed., *Ageing of composites*, Woodhead Publishing Limited and CRC Press, LLC **2008**, p. 3–33.
[18] A. R. Azura, S. Ghazali, M. Mariatti, *J. Appl. Polym. Sci.* **2008**, *110*, 747.
[19] S. S. Hamza, *Polym. Test* **1998**, *17*, 131.
[20] A. Choudhury, A. K. Bhowmick, M. Soddemann, *Polym. Degrad. Stab.* **2010**, *95*, 2555.
[21] D. Ruch, J. Exposito, C. Becker, F. Aubriet, *Surf. Interface Anal.* **2008**, *40*, 668.
[22] C. Saron, M. I. Felisberti, F. Zulli, M. Giordano, *J. Braz. Chem. Soc.* **2007**, *18*, 900.
[23] M. P. Scott, C. S. Brazel, M. G. Benton, J. W. Mays, J. D. Holbrey, R. D. Rogers, *Chem. Commun.* **2002**, *7*, 1370.
[24] J. Pernak, A. Czepukowicz, R. Prozniak, *Ind. Eng. Chem. Res.* **2001**, *40*, 2379.
[25] K. Subramaniam, A. Das, G. Heinrich, *Compos. Sci. Technol.* **2011**, *71*, 1441.
[26] A. Das, K. W. Stockelhuber, R. Jurk, J. Fritzsche, M. Kluppel, G. Heinrich, *Carbon* **2009**, *47*, 3313.
[27] K. Subramaniam, A. Das, D. Steinhauser, M. Klüppel, G. Heinrich, *Eur. Polym. J.* **2011**, *47*, 2234.
[28] M. Tunckol, J. Durand, Ph. Serp, *Carbon* **2012**, *50*, 4303.
[29] H. Kreyenschulte, S. Richter, T. Gotze, D. Fischer, D. Steinhauser, M. Kluppel, *Carbon* **2012**, *50*, 3649.
[30] Y. Lei, Z. Tang, L. Zhu, B. Guo, D. Jia, *Polymer* **2011**, *52*, 1337.
[31] Y.D. Lei, Z.H. Tang, B.C. Guo, L.X. Zhu, D.M. Jia, *Express Polym. Lett* **2010**, *4*, 692.
[32] K. Subramaniam, A. Das, L. Häußler Ch. Harnisch, K.W. Stöckelhuber, G. Heinrich, *Polym. Degrad. Stab.* **2012**, *97*, 776.
[33] K. Subramaniam, A. Das, G. Heinrich, *Compos. Sci. Technol.* **2013**, *74*, 14.
[34] A. Laskowska, A. Marzec, G. Boiteux, M. Zaborski, O. Gain, A. Serghei, *Polym. Int.* **2013**, *62*, 1575.
[35] P. J. Flory, J. Rehner, *J. Chem. Phys.* **1943**, *11*, 521.
[36] S. Thiruvarudchelvan, *J. Mater. Process. Technol.* **1993**, *39*, 55.
[37] H. W. Chou, J. S. Huang, *J Appl. Polym. Sci.* **2008**, *110*, 2907.
[38] L. Gonzalez, A. Rodriguez, J. L. Valentin, A. Marcos-Fernandez, P. Posadas, *Kautsch. Gummi Kunstst.* **2005**, *58*, 638.
[39] G. Mertz, F. Hassouna, P. Leclère, A. Dahoun, V. Toniazzo, D. Ruch, *Polym. Degrad. Stab.* **2012**, *97*, 2195.
[40] M. Guzzo, M. A. De Paoli, *Polym. Degrad. Stab.* **1992**, *38*, 41.
[41] M. C. S. Perera, U. S. Ishiaku, Z. A. M. Ishak, *Polym. Degrad. Stab.* **2000**, *68*, 393.
[42] J. Unsworth, Y. Li, *J. Appl. Polym. Sci.* **1992**, *46*, 1375.
[43] E. Marwanta, T. Mizumo, N. Nakamura, H. Ohno, *Polymer* **2005**, *46*, 3795.
[44] J. M. Pringle, J. Golding, C. M. Forsyth, G. B. Deacon, M. Forsyth, D. R. MacFarlane, *J. Mater. Chem.* **2002**, *12*, 3475.
[45] R. E. Panzer, M. J. Schaer, *J. Electrochem. Soc.* **1965**, *11*, 1136.
[46] F. Cataldo, *Polyhedron* **1992**, *1*, 79.

